Human P-Glycoprotein Exhibits Reduced Affinity for Substrates during a Catalytic Transition State†

Muralidhara Ramachandra,‡,§ Suresh V. Ambudkar,|| David Chen,‡,⊥ Christine A. Hrycyna,|| Saibal Dey,|| Michael M. Gottesman,|| and Ira Pastan*,‡

Laboratory of Molecular Biology and Laboratory of Cell Biology, Division of Basic Sciences, National Cancer Institute, National Institutes of Health, Bethesda, Maryland 20892

Received December 11, 1997; Revised Manuscript Received February 2, 1998

ABSTRACT: Human P-glycoprotein (Pgp), a plasma membrane protein that confers multidrug resistance, functions as an ATP-dependent drug efflux pump. Pgp contains two ATP binding/utilization sites and exhibits ATPase activity that is stimulated in the presence of substrates and modulating agents. The mechanism of coupling of ATP hydrolysis to drug transport is not known. To understand the role of ATP hydrolysis in drug binding, it is necessary to develop methods for purifying and reconstituting Pgp that retains properties including stimulation of ATPase activity by known substrates to an extent similar to that in the native membrane. In this study, $(His)_6$-tagged Pgp was expressed in *Trichoplusia ni* (High Five) cells using the recombinant baculovirus system and purified by metal affinity chromatography. Upon reconstitution into phospholipid vesicles, purified Pgp exhibited specific binding to analogues of substrates and ATP in affinity labeling experiments and displayed a high level of drug-stimulated ATPase activity (specific activity ranging from 4.5 to 6.5 μmol min^{-1} mg^{-1}). The ATPase activity was inhibited by ADP in a competitive manner, and by vanadate and *N*-ethylmaleimide at low concentrations. Vanadate which is known to inhibit ATPase activity by trapping MgADP at the catalytic site inhibited photoaffinity labeling of Pgp with substrate analogues, [^{125}I]iodoarylazidoprazosin and [^{3}H]azidopine, only under ATP hydrolysis conditions. Because vanadate-trapped Pgp is known to resemble the ADP and phosphate-bound catalytic transition state, our findings indicate that ATP hydrolysis results in a conformation with reduced affinity for substrates. A catalytic transition conformation with reduced affinity would essentially result in substrate dissociation and supports a model for drug transport in which an ATP hydrolysis-induced conformational change leads to drug release toward the extracellular medium.

Multidrug resistance, which is a major hurdle in successful cancer chemotherapy, is often associated with enhanced expression of the human multidrug resistance gene (*MDR*1) (*1, 2*). The *MDR*1 gene encodes a 170 kDa integral plasma membrane glycoprotein, termed P-glycoprotein (Pgp)[1] or the multidrug transporter. On the basis of its amino acid sequence, Pgp is predicted to consist of two similar halves, each containing six putative transmembrane segments and a nucleotide-binding domain (*3, 4*). These structural elements are shared by a large family of membrane transporters known as ATP−binding cassette (ABC) transporters (*4*).

Pgp utilizes the energy derived from ATP hydrolysis to transport a large number of structurally diverse cytotoxic drugs and other lipophilic compounds across the plasma membrane (*4*). Photoactive analogues of drugs, chemosensitizers, and ATP bind specifically to Pgp (*5*−*7*), and Pgp fails to transport drugs and confer resistance when mutations are introduced into either or both nucleotide-binding sites (*7*; C. A. Hrycyna et al., manuscript in preparation). Pgp exhibits both basal and substrate-stimulated ATPase activities, comparable to those of other transport ATPases, in crude membrane preparations and purified/reconstituted systems (*8*−*12*). Energy-dependent transport mediated by Pgp has been demonstrated in several systems, such as yeast secretory vesicles containing Pgp (*13*), mammalian cells transiently transfected with *MDR*1, without preexposure to cytotoxic drugs (*14*), membrane vesicles from multidrug resistant cells (*15*), and proteoliposomes containing purified Pgp (*16*−*18*).

The mechanism by which the energy derived from ATP hydrolysis is transduced into drug transport is not known. Photoaffinity labeling studies with drug analogues have identified two drug binding regions within the transmembrane domains of Pgp, one in each half of the molecule (*19*). Recent studies from our laboratory have demonstrated that these two photolabeled regions represent two nonidentical drug interaction sites (*20*). Unlike its binding to drugs, Pgp does

† C.A.H. is a fellow of The Jane Coffin Childs Memorial Fund for Medical Research.

* Corresponding author: Laboratory of Molecular Biology, Division of Basic Sciences, National Cancer Institute, Building 37, Room 4E16, National Institutes of Health, 37 Convent Dr., MSC 4255, Bethesda, MD 20892-4255. Telephone: (301) 496-4797. Fax: (301) 402-1344. E-mail: pasta@helix.nih.gov.

‡ Laboratory of Molecular Biology, National Cancer Institute.

§ Present address: Canji, Inc., 3030 Science Park Road, San Diego, CA 92121.

|| Laboratory of Cell Biology, National Cancer Institute.

⊥ Present address: Human Genetics Branch, National Institute of Child Health and Human Development, National Institutes of Health, Bethesda, MD 20892.

[1] Abbreviations: Pgp, P-glycoprotein; AMP−PNP, adenosine 5′-(β,γ-imino)triphosphate; IAAP, [^{125}I]iodoarylazidoprazosin; TAMA, [^{3}H]tamoxifen aziridine.

S0006-2960(97)03045-6
Published on Web 03/17/1998

not interact with nucleotides with high affinity (*21*). Vanadate, a potent inhibitor of Pgp-ATPase activity (*8, 9*) and transport function (*15*), greatly increases the apparent affinity for MgADP by blocking its release from the catalytic site (*21*), and this stably inhibited complex resembles the normal catalytic transition state in which phosphate and MgADP are bound and subsequently released (*21, 22*). When vanadate is present, only a single turnover of the enzyme occurs as a result of trapping. Vanadate-trapping experiments have confirmed earlier findings that both nucleotide binding sites are catalytically active (*23*) and suggested that the two nucleotide sites may alternate in catalysis (*22, 24*). A detailed characterization of the vanadate-trapped species using purified Pgp, which is devoid of other ATPases and ATP-binding proteins, might provide further insights into the mechanism by which ATPase activity is coupled to drug transport.

In this study, $(His)_6$-tagged Pgp expressed using the recombinant baculovirus system was purified rapidly and efficiently by metal affinity chromatography. The catalytic properties of the purified and reconstituted Pgp preparation were similar to the properties of that in crude membranes, indicating that the native conformation and function of the protein were preserved during purification. Characterization of the effects of nucleotide binding and hydrolysis on interaction with substrate analogues revealed that Pgp exhibits drastically reduced affinity for substrates upon ATP hydrolysis in the presence of vanadate. Since the vanadate-trapped complex is known to mimic Pgp−MgADP−phosphate, our results show that Pgp exhibits reduced affinity for substrates during a catalytic transition state.

MATERIALS AND METHODS

Cell Lines and Viruses. Trichoplusia ni (High Five) (HF) cells obtained from Invitrogen (San Diego, CA) were propagated as monolayer cultures at 27 °C in serum-free ExCell 400 (JRH Biosciences, Lenexa, KS) medium supplemented with antibiotic−antimycotic (Life Technologies, Grand Island, NY). *Spodoptera frugiperda* (Sf9) cells were grown as monolayer cultures at 27 °C in Grace's medium (Life Technologies) with 10% fetal bovine serum (Life Technologies) and antibiotic−antimycotic.

Generation of Recombinant Baculovirus Encoding $(His)_6$-tagged Pgp. Standard recombinant DNA procedures were used to construct the transfer vector pBacPAK-MDR1(H_6) encoding $(His)_6$-tagged human *MDR*1. The sequence encoding $(His)_6$ followed by a termination codon was inserted at the 3′ end of the *MDR*1 cDNA using a PCR-based protocol. The modified *MDR*1 cDNA was subcloned into plasmid pBacPAK 9 (Clontech, Palo Alto, CA) to obtain the transfer vector pBacPAK-MDR1(H_6). Introduction of a convenient restriction enzyme site for subcloning purposes resulted in insertion of an additional sequence that codes for amino acids Leu and Ala before the $(His)_6$ tag. Recombinant baculovirus encoding $(His)_6$-tagged human wild-type *MDR*1 was then generated by cotransfection of Sf9 cells with the transfer plasmid and BacPAK6 DNA (*Bsu36* I digest) (Clontech). After transfection, recombinant plaques were isolated from the culture supernatant by following the protocols recommended by Clontech.

Expression of Pgp. Insect cells grown in T162-cm^2 tissue culture flasks (2×10^7 cells/flask) were infected with BV-MDR1(H_6) at a multiplicity of infection of 10 for 2 h in 4 mL of Ex-Cell 400 medium for HF cells and Grace's medium supplemented with fetal bovine serum for Sf9 cells. After 2 h, cells were fed with 16 mL of the respective media and incubated at 27 °C for 3 days.

Preparation of Crude Membranes. Crude membranes from insect cells were prepared as described (*8*) with some modifications. Cells were incubated on ice for 45 min in a lysis buffer containing 50 mM Tris-HCl (pH 7.5), 50 mM mannitol, 2 mM EGTA, 2 mM dithiothreitol, 1 mM 4-(2-aminoethyl)benzenesulfonyl fluoride (AEBSF), and 1% aprotinin (Sigma, Catalog no. A6279) and subsequently disrupted using a Dounce homogenizer (30 strokes with pestle A). The undisrupted cells and nuclear debris were removed by centrifugation at 500*g* for 10 min. The low-speed supernatant was diluted 2-fold in resuspension buffer containing 50 mM Tris-HCl (pH 7.5), 300 mM mannitol, 1 mM EGTA, 1 mM dithiothreitol, 1 mM AEBSF, and 1% aprotinin. The membranes were collected by centrifugation for 60 min at 100000*g* and resuspended in resuspension buffer containing 10% glycerol. The resuspended membranes were stored in small aliquots at −70 °C. The protein content was determined by a modified Lowry method (*25*), using bovine serum albumin as a standard.

Solubilization of Pgp. Membranes prepared from insect cells were solubilized using octyl β-D-glucopyranoside (octyl glucoside from Calbiochem, San Diego, CA) as described (*9*) with modifications. Crude membranes were resuspended at 2.0 mg/mL in 20 mM Tris-HCl (pH 8.0), 20% glycerol, 150 mM NaCl, 2 mM β-mercaptoethanol, a 0.4% lipid mixture consisting of *Escherichia coli* bulk phospholipid, phosphatidylcholine, phosphatidylserine, and cholesterol (all from Avanti Polar Lipids, Alabaster, AL) at 60:17.5:10:12.5 (w/w), respectively, 2.0% octyl glucoside, 1.5 mM $MgCl_2$, 1 mM AEBSF, 2 μg/mL pepstatin, 2 μg/mL leupeptin, and 1% aprotinin and incubated on ice for 20 min. After 20 min, insoluble material was removed by centrifugation at 100000*g* for 1 h.

Purification of Pgp by Metal Affinity Chromatography. After imidazole was added at a final concentration of 2 mM, the detergent extract (10 mg of protein) was incubated for 30 min at 4 °C on a rotary shaker with 0.5 mL of Talon metal affinity resin (Clontech) that was prewashed once with buffer A composed of 20 mM Tris-HCl (pH 8.0), 100 mM NaCl, 20% glycerol, 2.5 mM β-mercaptoethanol, a 0.1% lipid mixture (same as above), 1.25% octyl glucoside, 1 mM $MgCl_2$, 1 mM AEBSF, 2 μg/mL pepstatin, 2 μg/mL leupeptin, and 1% aprotinin. The metal affinity beads were pelleted by centrifugation for 5 min at 500*g* and washed twice by resuspending and incubating in 10 mL of buffer A at 4 °C for 10 min on a rotary shaker. The beads were then resuspended in 1 mL of buffer A and applied to a 4 mL disposable column (Bio-Rad, Hercules, CA). After being washed twice in 5 mL of buffer A containing 500 mM KCl, proteins were eluted stepwise in 2 mL each of buffer B (same as buffer A except with 20 mM Tris-HCl at pH 6.8 instead of at pH 8.0) containing 10, 100, and 200 mM imidazole. Fractions eluted from the column were concentrated using Centriprep-50 concentrators (Amicon, Beverly, MA) and stored in aliquots at −70 °C.

SDS−Polyacrylamide Gel Electrophoresis (SDS−PAGE) and Immunoblot Analysis. SDS−PAGE and immunoblot analysis were performed as described (*26*).

Photoaffinity Labeling. Affinity labeling of Pgp in crude membranes or purified preparations was performed with either [^{125}I]iodoarylazidoprazosin (IAAP; specific activity of 2200 Ci/mmol, NEN, Boston, MA), [^{3}H]azidopine (specific activity of 46 Ci/mmol, Amersham, Arlington Heights, IL), or [^{3}H]tamoxifen aziridine (TAMA) (specific activity of 30 Ci/mmol, Amersham). Crude membranes (10 μg) were diluted in an assay buffer containing 10 mM Tris-HCl (pH 7.0), 150 mM NaCl, and 250 mM sucrose, whereas purified Pgp (~1 μg) was first diluted in a reaction mixture (20-fold dilution in a final volume of 50 μL) containing 50 mM Tris-HCl (pH 7.0), 125 mM KCl, and 1 mM dithiothreitol and incubated at room temperature for 5 min. Then either 4 nM [^{125}I]IAAP, 0.4 μM [^{3}H] azidopine, or 0.8 μM [^{3}H]TAMA was added, and samples were incubated in the dark at 37 °C for 10 min. To study vanadate-induced inhibition of drug binding, vanadate, nucleotides, and $MgCl_2$ were added to the reaction mixtures at the indicated concentrations prior to the addition of radiolabel and incubated at the indicated temperatures. After 10 min, samples with IAAP and azidopine were exposed to a UV lamp (Black-Ray lamp, 365 nm wavelength, UVP, Uplard, CA) on ice for 30 min. For TAMA labeling, samples were incubated at room temperature in the dark for 30 min. Samples were then subjected to SDS−PAGE and autoradiography. The signals on dried gels containing ^{125}I-labeled samples were quantitated using the Storm System (Molecular Dynamics, Sunnyvale, CA), whereas signals on the autoradiograms obtained for ^{3}H-labeled samples were quantitated using NIH Image software after capturing the images on a Macintosh computer using the Eagle Eye still video system (Stratagene, La Jolla, CA).

For 8-azidoATP labeling, purified Pgp preparations (~1 μg) were diluted 20-fold in a 50 μL reaction mixture containing 50 mM Tris-HCl (pH 7.0), 125 mM KCl, 10 mM $MgCl_2$, and 1 mM dithiothreitol, and incubated at room temperature for 5 min. Samples were then chilled by incubating for 3 min on ice, and 2.5 μM [α-^{32}P]-8-azidoATP (specific activity of 9.60 Ci/mmol, ICN Biomedicals) was added. After a 10 min incubation on ice, samples were exposed to UV light at 365 nm on ice for 20 min and subjected to SDS−PAGE and autoradiography.

Measurement of ATPase Activity. Pgp-associated ATPase activity in crude membranes was determined as the vanadate-sensitive release of inorganic phosphate from Mg^{2+}ATP as described (*8*). To assay the activity in purified Pgp preparations, a solubilized and purified preparation (~1 μg in a 5 μL volume) containing 1.25% octyl glucoside and a 0.1% lipid mixture was first diluted about 20-fold in a reaction mixture (100 μL final volume) containing 50 mM Tris-HCl (pH 7.0), 125 mM KCl, and 1 mM dithiothreitol and incubated at 37 °C for 5 min. The drugs were added from stock solutions prepared in dimethyl sulfoxide (final concentration of dimethyl sulfoxide at 1%), and the assay mixtures were then incubated for 3 min at 37 °C. The reactions were started by the addition of 2.5 mM ATP and 5 mM $MgCl_2$, and the mixtures were incubated at 37 °C for desired periods of time. After the reactions were stopped by the addition of 100 μL of a 5% SDS solution, the amount of phosphate released was measured as described (*8*).

RESULTS

Introduction of the $(His)_6$ Tag at the C Terminus of Pgp. To purify Pgp rapidly under relatively mild conditions, we sought to utilize an affinity tag consisting of six histidine residues. Purification of Pgp consisting of 10 histidine residues at the C terminus with drug-stimulated ATPase activity has already been reported (*23*). However, possible interference of the tag with its transport function was not studied. Using a vaccinia virus-based transient Pgp expression system (*14*), untagged and tagged variants of Pgp were expressed in HeLa cells and possible effects of the $(His)_6$ tag on Pgp expression and function were assessed. Staining cells with MRK-16, a monoclonal antibody that recognizes an external epitope of human Pgp (*27*), and analysis by fluorescence activated cell sorting (FACS) showed that both the wild-type and $(His)_6$-tagged Pgps were localized to the cell surface to a similar extent (M. Ramachandra et al., unpublished results). In FACS assays, the $(His)_6$-tagged Pgp was as efficient as the untagged Pgp in transporting rhodamine 123, a known Pgp substrate. Transport of Rhodamine 123 was reversed in the presence of verapamil or cyclosporin A to a similar extent, indicating that introduction of the $(His)_6$ tag does not alter the transport function of Pgp and its interaction with known modulators (M. Ramachandra et al., unpublished results).

Expression of Pgp of High Specific ATPase Activity in HF Cells. To express and purify large amounts of protein, recombinant baculovirus encoding $(His)_6$-tagged Pgp was generated. Although a relatively high level of expression was achieved in Sf9 cells (3−4% of the total membrane protein), vanadate-sensitive Pgp-ATPase activity in the crude membranes prepared from these cells was much lower [40−70 nmol hydrolyzed min^{-1} mg^{-1} protein)] (Figure 1A) than that reported in earlier studies (*8*). Several other reports indicate that the common practice of Pgp expression in Sf9 cells using recombinant baculoviruses yields protein with drug-stimulated ATPase activity that is highly variable from batch to batch as well as from laboratory to laboratory [for example, a specific activity of 40−50 nmol min^{-1} mg^{-1} (*28*) as compared to 150 nmol min^{-1} mg^{-1} (*8*)]. Therefore, we then utilized HF cells for Pgp expression using recombinant baculoviruses. Immunoblot analysis of the crude membranes from infected cells showed that expression of Pgp was similar to that obtained in Sf9 cells (Figure 1A). However, when crude membranes from BV-MDR1(H_6)-infected HF cells were assayed for ATPase activity, a consistently higher level of activity (125−175 nmol hydrolyzed min^{-1} mg^{-1}) was obtained (Figure 1). Maximum Pgp-ATPase activity was obtained in membranes isolated from cells harvested 3 days postinfection (Figure 1B). Similar levels of Pgp-ATPase activities were observed when HF cells were cultured in the presence or absence of fetal bovine serum. Control membranes prepared from uninfected HF cells did not show any endogenous Pgp expression in immunoblot analysis and did not exhibit drug-stimulated ATPase activity.

Purification of Pgp by Metal Affinity Chromatography. Pgp in crude membranes isolated from HF cells was solubilized using octyl glucoside in the presence of a lipid mixture consisting of *E. coli* bulk phospholipid, phosphatidylcholine, phosphatidylserine, and cholesterol at 60:17.5:10:12.5 (w/w). The use of octyl glucoside and the lipid

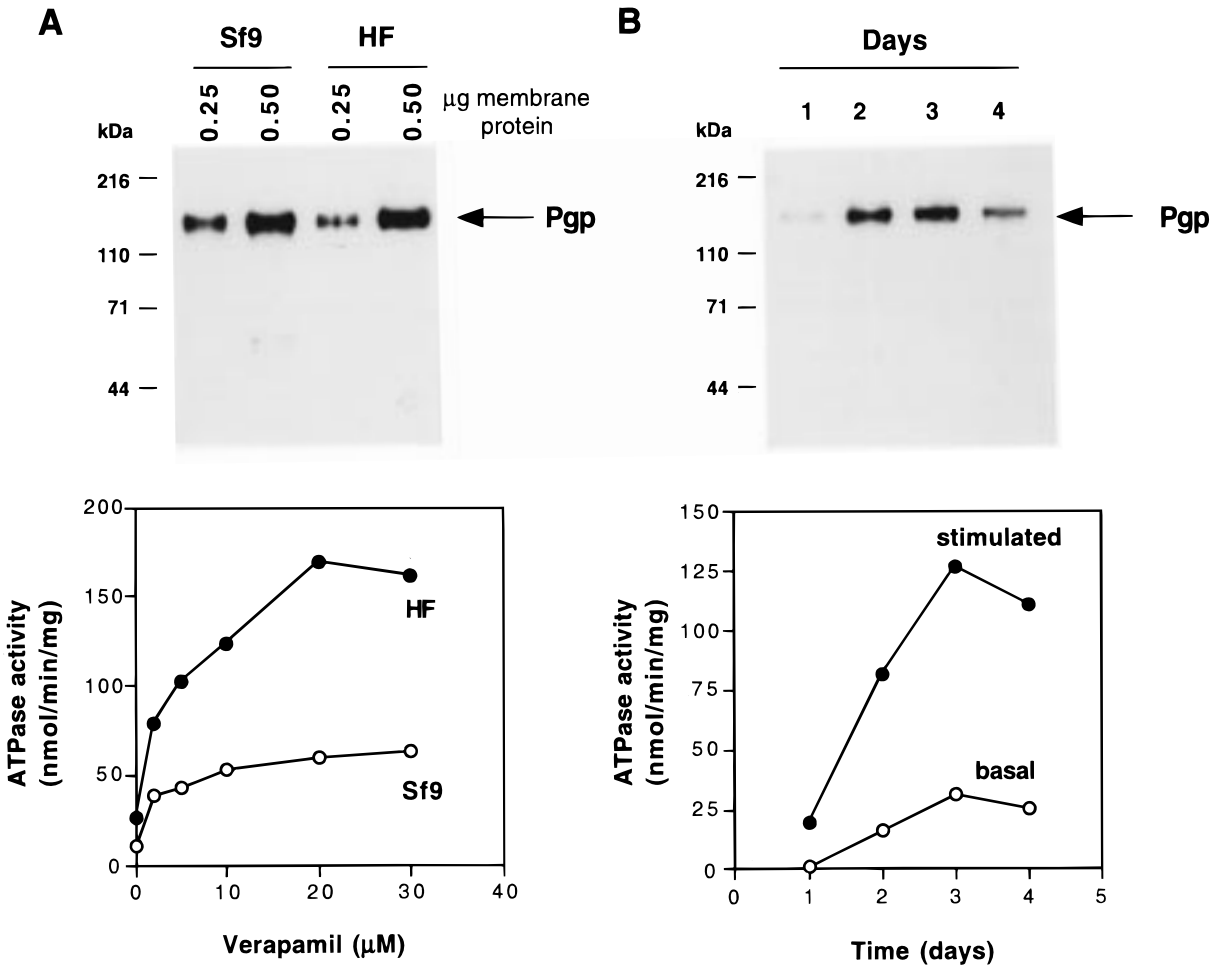

FIGURE 1: Expression of $(His)_6$-tagged Pgp of high specific drug-stimulated ATPase activity. (A) HF (•) and Sf9 (○) cells were infected with BV-MDR1(H_6) and harvested 3 days after infection. Crude membranes were isolated and analyzed for Pgp expression by immunoblot analysis (top) using anti-Pgp monoclonal antibody C219 (amounts of total membrane protein used are indicated) and for the vanadate-sensitive ATPase activity in the presence of varying concentrations of verapamil (bottom). (B) HF cells were infected with BV-MDR1(H_6) and harvested at various time points after infection (days after infection are indicated). Crude membranes were isolated and analyzed for Pgp expression by immunoblot analysis using C219 (0.25 μg of membrane protein per lane) (top) and ATPase activity (bottom) in the presence (●) or absence (○) of 30 μM verapamil.

mixture for solubilization and purification was based on earlier studies that have established that functional properties of Pgp are retained under these conditions (*9*, *11*, *16*). Solubilized $(His)_6$-tagged Pgp was purified by Talon metal affinity chromatography using imidazole-containing buffers for elution of bound proteins. As shown in Figure 2, a one-step purification yielded Pgp that was about 85% pure in fractions eluted with 100 mM imidazole. Using this protocol, we were able to purify up to 1.0 mg of Pgp from 3×10^8 HF cells grown as a monolayer culture in serum-free medium. As the 100 mM imidazole fraction contains the most pure Pgp, we have used this fraction for the experiments described in Figures 4−6.

Purified Pgp Exhibits Specific Binding to Analogues of Drugs and ATP. Since purified Pgp preparations contained a 0.1% lipid mixture and 1.25% octyl glucoside (about twice the critical micellar concentration), we reasoned that simple dilution of these preparations should reduce the final detergent concentration to a point where the lipids and protein spontaneously vesiculate. Such virtually instantaneous reconstitution of octyl glucoside-solubilized membrane proteins into liposomes by dilution into assay buffers has been performed earlier (*29*−*31*). The purified Pgp was diluted 20-fold in the assay buffer, and drug binding properties were determined in affinity labeling experiments. Centrifugation of the diluted samples in parallel experiments for 1 h at 100000*g*, yielded 17−20% of the input Pgp in pellets, suggesting that about one-fifth of the input Pgp was reconstituted in lipid vesicles. As shown in Figure 3A, when diluted in the assay buffer, purified Pgp exhibited specific binding to IAAP, azidopine, and TAMA. Affinity labeling of Pgp did not occur when octyl glucoside was included at 1.25% in the assay buffer, indicating that solubilized Pgp does not bind drugs. Affinity labeling of Pgp with all three substrate analogues was competed for by vinblastine and cyclosporin A, confirming the specificity of the cross-linking reactions. Upon dilution in a detergent-free buffer, purified Pgp also exhibited specific binding to the photoactive ATP analogue, 8-azidoATP (Figure 3B). For 8-azidoATP binding, the presence of Mg^{2+} was absolutely necessary and the cross-linking was effectively competed for by ATP and ADP (Figure 3B). Incubation at 37 °C or on ice with 200 μM vanadate did not show any marked effect on labeling, indicating that vanadate has no effect on reconstitution and interaction of Pgp with the ATP analogue (Figure 3B). It should be noted that, since purified Pgp was used for

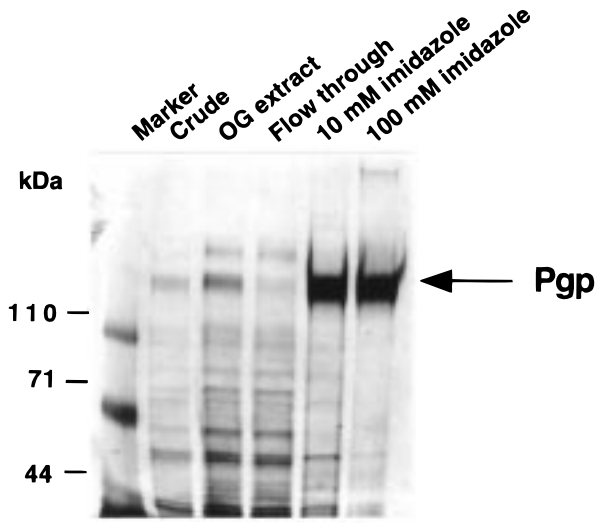

FIGURE 2: Purification of Pgp. Crude membranes from HF cells infected with BV-MDR1(H_6) were solubilized using octyl glucoside (OG) as described in Materials and Methods, and Pgp from solubilized extract was purified by Talon metal affinity chromatography (Clontech). Bound proteins from the column were eluted with buffers containing imidazole. Samples from different steps of purification (2.0 μg of protein/lane) were subjected to SDS−PAGE and silver staining.

labeling, unbound ligands, including vanadate and 8-azidoATP, were not removed before UV cross-linking (Figure 3B). Removal of unbound ligands after preincubation with vanadate and 8-azidoATP, but prior to UV cross-linking, has been shown to result in specific labeling of Pgp in crude membrane preparations (*21*).

Purified Pgp Exhibits a High Level of Drug-Stimulated ATPase Activity. In keeping with earlier studies (*9*), solubilized Pgp did not show any drug-stimulated ATPase activity. Upon reconstitution, both basal and drug-stimulated ATPase activities of the protein were regenerated. Alamethicin, a compound known to permeabilize proteoliposomes, increased ATPase activity of Pgp in a dose-dependent manner up to 0.1 μg/μL. At 0.1 μg/μL alamethicin, there was nearly a 2-fold increase in ATPase activity, suggesting that about 50% of the catalytically active Pgp molecules are inserted into proteoliposomes in an inside-out orientation. Therefore, the fraction reconstituted in an inside-out orientation was taken into consideration while calculating ATPase activity per milligram of purified protein.

Purified Pgp showed a basal activity of 1.0−1.8 μmol min^{-1} (mg of protein)$^{-1}$ that was stimulated in the presence of known substrates (Figure 4A and Table 1). Verapamil stimulated the ATPase activity in a dose-dependent manner and a maximum activity of 4.5−6.5 μmol min^{-1} (mg of Pgp)$^{-1}$ was obtained (Figure 4A). In addition to verapamil, other compounds, including vinblastine, nicardipine, tamoxifen, bisantrene, tetraphenylphosphonium, and prazosin, stimulated Pgp-ATPase activity (Table 1). Maximum stimulation of about 4.5-fold was observed with prazosin. Cyclosporin A, a known inhibitor of Pgp, showed no effect on the basal ATPase activity, but inhibited the verapamil-stimulated activity, with an IC_{50} value of 210 nM. Determination of ATPase activity as a function of ATP concentration indicated that the reaction follows Michaelis−Menton kinetics with a K_m of 0.6 mM. In the presence of 30 μM verapamil, the apparent K_m for ATP remained the same, revealing that drug binding does not alter the affinity for ATP (*9*). ATPase activity of the purified Pgp was inhibited by ADP in a competitive manner with a K_i of 0.3 mM. Vanadate and *N*-ethylmaleimide inhibited Pgp-ATPase activity with IC_{50} values of 2 and 35 μM, respectively. Like the results of several earlier studies, inhibitors of other ATPases such as ouabain, EGTA, and sodium azide did not inhibit Pgp-ATPase activity up to concentrations of 1, 2, and 5 mM, respectively.

Effect of Vanadate-Induced Nucleotide Trapping on Drug Binding. The results described above showed that the properties of purified and reconstituted Pgp are similar to those seen in crude membranes, indicating that the native structure of the protein is preserved during purification and reconstitution. We reasoned that since the purified preparation exhibited a high level of drug-stimulated ATPase activity upon reconstitution that was inhibited at low concentrations of vanadate, it would be an excellent system for studying the nature of coupling of ATP hydrolysis to drug binding using the vanadate-trapping technique. As shown in Figure 5A, ATP or ADP did not show any marked effect on labeling with IAAP, a photoactive analogue of prazosin, under ATP hydrolysis conditions at 37 °C or on ice (1 °C) (data not shown). However, in the presence of $MgCl_2$ and ATP at 37 °C (ATP hydrolysis conditions), but not at 1 °C, vanadate inhibited IAAP labeling in a concentration-dependent manner (Figure 5B,C). Immunoblot analysis of aliquots from similarly treated samples indicated that the inhibition is not due to Pgp degradation. When the effect of vanadate on ATPase activity was determined under similar conditions, but with 30 μM verapamil instead of IAAP, inhibition of ATPase activity by vanadate was parallel to vanadate-induced inhibition of IAAP labeling (Figure 5C). To correct for the presence of Pgp molecules that do not participate in ATP hydrolysis, IAAP labeling values obtained after subtraction of the residual labeling in the presence of 400 μM vanadate, a concentration at which ATPase activity was completely inhibited, from the amount of labeling at different vanadate concentrations were plotted (Figure 5C). As expected, ATP was not hydrolyzed at 1 °C (data not shown). Vanadate addition did not result in diminished IAAP labeling when $MgCl_2$ or ATP was excluded from the reaction mixture (Figure 6A). Furthermore, vanadate-induced inhibition did not occur when ATP was replaced with either ADP or AMP−PNP (Figure 6B). These results demonstrate that ATP hydrolysis is essential for inhibition of IAAP labeling resulting from vanadate-induced nucleotide trapping. Similar vanadate-induced inhibition of IAAP labeling of Pgp was also observed in crude membrane preparations from either insect or mammalian cells (see below), indicating that vanadate-induced inhibition of drug binding is not an artifact of the purified/reconstituted system. Moreover, vanadate-induced inhibition of photoaffinity labeling of Pgp with azidopine was also observed under ATP hydrolysis conditions in crude membrane preparations from insect (Figure 6C) or *MDR*1-transfected and vincristine-selected NIH3T3 (N3-2400) (*26*) cells (M. Ramachandra et al., unpublished results).

DISCUSSION

Purification and Functional Reconstitution of Human Pgp Expressed in Insect cells Using the Baculovirus System. To

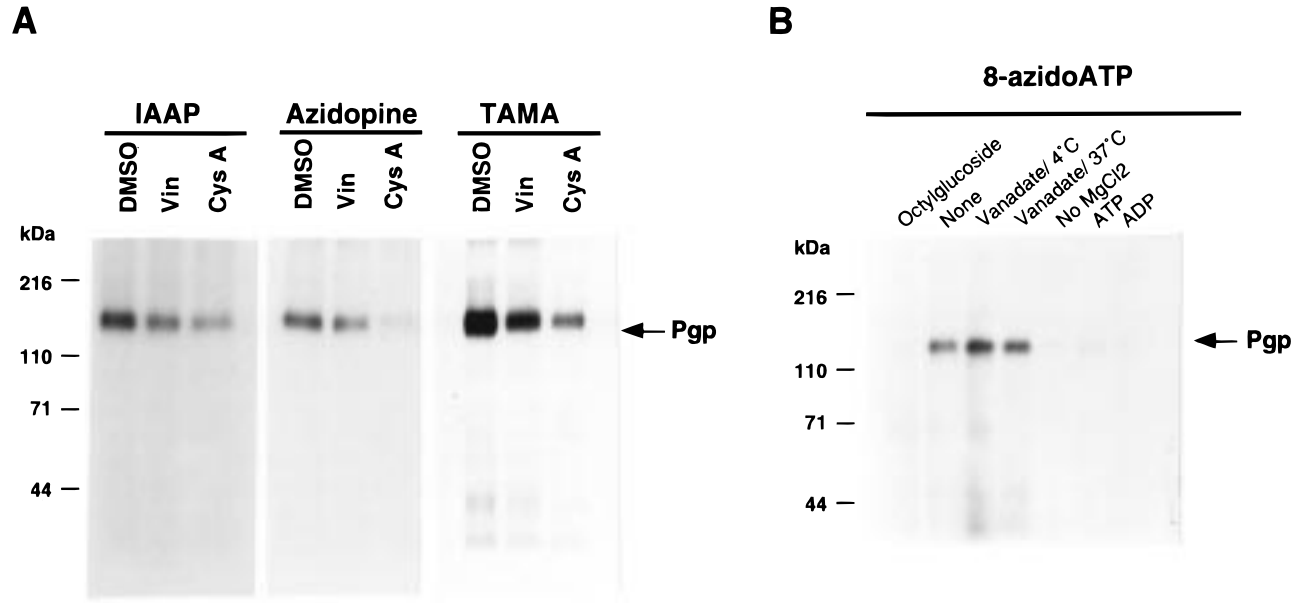

FIGURE 3: Affinity labeling of purified Pgp with analogues of drugs and ATP. (A) Purified Pgp was labeled with substrate analogues, [^{125}I]IAAP, [^{3}H]azidopine, and [^{3}H]TAMA and analyzed by SDS−PAGE and autoradiography. Where indicated, vinblastine (Vin) and cyclosporin A (Cys A) as competitors at 25 and 10 μM, respectively, and dimethyl sulfoxide (DMSO) as a control were added. (B) Purified Pgp was photoaffinity labeled with [α-^{32}P]-8-azidoATP in 50 mM Tris-HCl (pH 7.0), 125 mM KCl, 5 mM $MgCl_2$, and 1 mM dithiothreitol as described in Materials and Methods. Variations to the standard protocol are indicated above each lane: in the presence of octyl glucoside (1.25% final), without any modification (none), with 200 μM vanadate at 4 °C (vanadate/4 °C), with 200 μM vanadate at 37 °C (vanadate/37 °C), without $MgCl_2$ (no $MgCl_2$), with 100 μM ATP (ATP), and with 100 μM ADP (ADP).

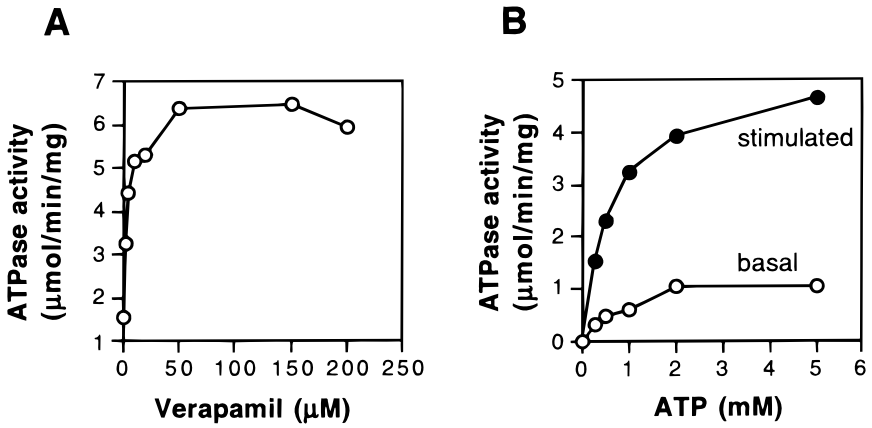

FIGURE 4: ATPase activity of purified Pgp. ATPase activity of purified Pgp was assayed as described in Materials and Methods. (A) ATPase activity was determined at varying concentrations of verapamil, 2.5 mM ATP, and 5 mM $MgCl_2$. (B) ATPase activity was measured as a function of ATP concentration with a constant molar ratio of ATP:Mg^{2+} of 1:2 and with (●) or without (○) 30 μM verapamil.

Table 1: Effects of Selected Compounds on ATPase Activity of Purified Pgp[a]

compound	concentration required for half-maximal stimulation (μM)	maximal stimulation (-fold)
verapamil	2.9	4.2
nicardipine	2.0	3.6
vinblastine	1.0	2.0
bisantrene	9.6	2.9
tamoxifen	10.0	2.2
tetraphenylphosphonium	22.0	3.8
prazosin	22.0	4.5

[a] Purified Pgp was reconstituted into phospholipid vesicles by 20-fold dilution in the assay buffer, and the vanadate-sensitive ATPase activity was measured as described in Materials and Methods. For each drug, at least five concentrations were used to determine these values.

examine the role of ATP hydrolysis in drug binding, it was essential to establish optimum conditions for purification and reconstitution for obtaining a Pgp preparation that retains the ability to interact with drugs and nucleotides similar to that in the native membrane. $(His)_6$-tagged Pgp of high specific ATPase activity (Figure 1) expressed in HF cells was purified by Talon metal affinity chromatography (Figure 2). To assess the properties of purified Pgp, we utilized a simplified procedure for reconstitution. Purified Pgp in 1.25% octyl glucoside and a 0.1% lipid mixture was diluted 20-fold in the assay for photoaffinity labeling and measurement of ATPase activity. The protein-to-lipid ratio in the purified material used for reconstitution was less than 1:25 (w/w). Purified/reconstituted Pgp exhibited specific binding to substrate and ATP analogues in photoaffinity labeling experiments (Figure 3) and displayed a high level of drug-stimulated ATPase activity (Figure 4). Verapamil-stimulated ATPase activity of 5−6 μmol min^{-1} (mg of protein)$^{-1}$ is in agreement with earlier estimates of 3−5 μmol min^{-1} (mg of protein)$^{-1}$ based on the content and specific activity in crude membrane preparations (*8*). The concentrations re-

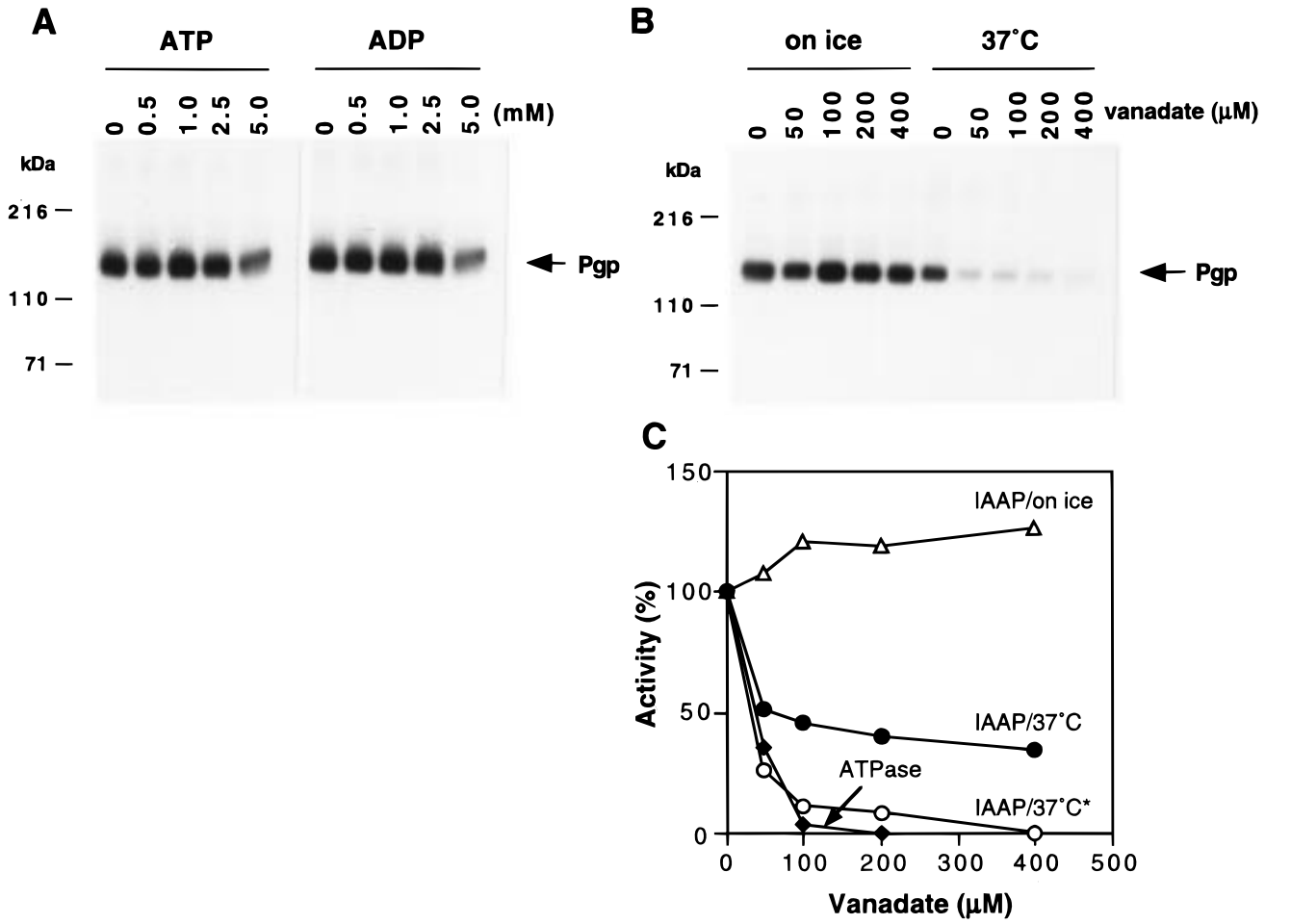

FIGURE 5: Effect of vanadate-induced nucleotide trapping on IAAP labeling and ATPase activity of purified Pgp. Photoaffinity labeling of purified Pgp was performed as described in Materials and Methods. (A) After dilution of purified Pgp in 50 mM Tris-HCl (pH 7.0), 125 mM KCl, and 1 mM dithiothreitol and incubation at room temperature for 5 min, 5 mM $MgCl_2$, ATP or ADP at indicated concentrations, and 4 nM IAAP were added and the mixture was incubated at 37 °C. After a 10 min incubation, samples were exposed to UV on ice for 30 min and analyzed by SDS−PAGE and autoradiography. (B) Purified Pgp was photoaffinity labeled with IAAP as described above, but in the presence of 2.5 mM ATP and varied concentrations of vanadate either at 37 °C or on ice. Photolabeled samples were subjected to SDS−PAGE and autoradiography. (C) In a parallel experiment, ATPase assays were performed at 37 °C under similar conditions but with 30 μM verapamil instead of IAAP. After a 10 min incubation at 37 °C, reactions were terminated and the amount of phosphate released was determined. The ATPase activity (◆) is plotted along with the percentage of IAAP labeling at 37 °C (IAAP/37 °C, ●) or on ice (IAAP/on ice, △) calculated after quantitating the radioactivity associated with each band shown in panel B. The percentage of IAAP labeling values obtained after subtraction of the residual labeling in the presence of 400 μM vanadate, a concentration at which ATPase activity was completely inhibited, from the amount of labeling at different vanadate concentrations are also plotted (IAAP/37 °C*, ○) to indicate that inhibition of ATPase activity is parallel with inhibition of IAAP labeling.

quired for half-maximal stimulation (Table 1) or inhibition with various substrates and inhibitors and K_m for ATP and K_i for ADP determined for purified/reconstituted Pgp were similar to those in the crude plasma membrane preparations, demonstrating that the native structure of the protein is preserved during purification and reconstitution.

Effect of Vanadate-Induced Nucleotide Trapping on Drug Binding Properties of Pgp. Studies from Senior's laboratory have elegantly shown that, upon trapping of vanadate at the catalytic site, the binding affinity for nucleotide increases dramatically and the resulting Pgp−MgADP−vanadate complex has a significantly longer half-life than the Pgp−MgADP−phosphate intermediate (*21*, *22*). Thus, the vanadate-trapping technique is an excellent tool for assessing the effects of binding of nucleotides at physiological concentrations. In an earlier study, Urbatsch and Senior (*32*) had observed a considerable reduction in the amount of azidopine labeling of Pgp in crude membranes from colchicine-resistant Chinese hamster ovary cells in the presence of several catalytic ligands, including ATP and vanadate. They suggested that photolabeling in the presence of catalytic ligands is potentially valuable as an assay of coupling between catalytic sites and drug binding sites of Pgp. However, precise conditions for the inhibition of azidopine labeling and the role of ATP hydrolysis in this inhibition were not established.

We used purified Pgp that is devoid of other ATPases and ATP-binding proteins to provide important insights into coupling between ATP hydrolysis and drug binding and/or transport. It is evident from several findings that, during affinity labeling with IAAP, it binds to Pgp in a manner analogous to that of known transport substrates and chemosensitizers. IAAP binds to Pgp in a saturable manner (*20*), and thus, it is one of the better affinity labels for studying drug binding properties of Pgp. IAAP binds to purified and reconstituted Pgp, which is competed for by vinblastine and

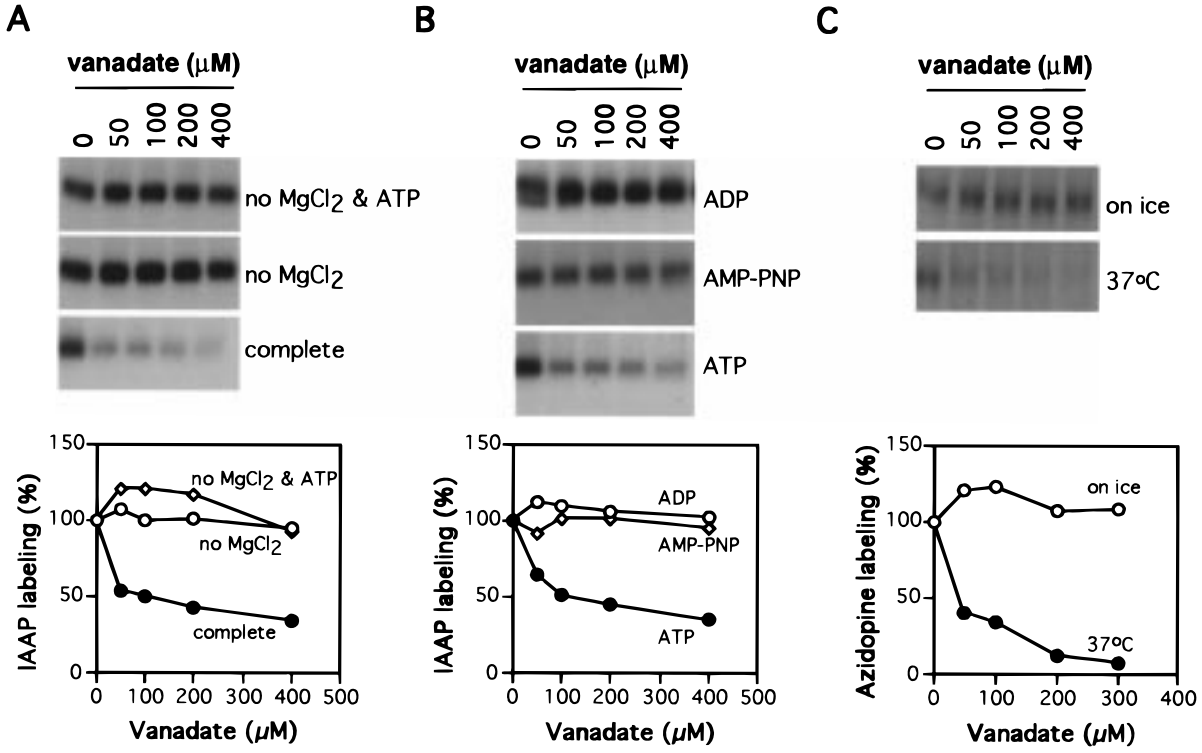

FIGURE 6: Pgp-mediated ATP hydrolysis is essential for vanadate-induced inhibition of IAAP and azidopine labeling. (A) IAAP labeling of purified Pgp was performed with varying concentrations of vanadate as indicated in Figure 5 and without both $MgCl_2$ and ATP (◇), without $MgCl_2$ but with 2.5 mM ATP (○), and with 5 mM $MgCl_2$ and 2.5 mM ATP (●). After labeling, samples were analyzed by SDS−PAGE and autoradiography. Radioactivity associated with each band (top) was quantitated and plotted (bottom). (B) The effect of vanadate on IAAP labeling was determined in photoaffinity experiments in the presence of varying concentrations of vanadate, 5 mM $MgCl_2$, and 2.5 mM of either ATP (●), ADP (○), or AMP−PNP (◇). (C) The effect of vanadate on photoaffinity labeling of Pgp with azidopine in crude membrane preparations from BV-MDR1(H_6)-infected HF cells was determined after preincubating in the presence of varying concentrations of vanadate, 10 mM $MgCl_2$, and 5 mM ATP at 37 °C (●) or on ice (○).

cyclosporin A (Figure 3A), and its parent compound, prazosin, stimulates Pgp-ATPase activity by about 4.5-fold (Table 1). In addition to vinblastine and cyclosporin A, a number of other known substrates and reversing agents compete for the binding of IAAP to Pgp in crude membranes (M. Ramachandra et al., unpublished results). IAAP does not label *MDR*2 (*20*), a closely related protein that functions as a phosphatidylcholine translocase. Additionally, bodipy FL-prazosin, a fluorescent derivative of prazosin, has been shown to be transported by Pgp in *MDR*1-transfected NIH3T3 cells (*20*).

In photoaffinity labeling experiments with purified and reconstituted Pgp, neither ATP nor ADP showed any noticeable effect on IAAP labeling (Figure 5A), which is consistent with earlier findings showing that Pgp does not have a high-affinity nucleotide binding site, and drugs can bind to Pgp in the absence of nucleotide binding and hydrolysis. Vanadate inhibited IAAP labeling in a concentration-dependent manner, when incubated in the presence of $MgCl_2$ and ATP at 37 °C (Figure 5B), but not on ice. The presence of Mg^{2+} and ATP was essential for vanadate-induced inhibition of IAAP labeling (Figure 6A). Inhibition did not occur when ATP was replaced with either ADP or AMP−PNP (Figure 6B). Moreover, vanadate-induced inhibition of IAAP labeling was parallel to the inhibition of Pgp-ATPase activity (Figure 5C). These results clearly show that ATP hydrolysis is essential for inhibition of IAAP labeling as a result of vanadate-induced nucleotide trapping. Furthermore, vanadate-induced inhibition of photoaffinity labeling did not occur in Pgp mutants incapable of binding and/or hydrolyzing ATP because of point mutation(s) in either N, C, or both nucleotide binding/utilization sites (M. Ramachandra et al., unpublished results). Additionally, photoaffinity labeling of Pgp with azidopine in crude membrane preparations was also inhibited by vanadate in a concentration-dependent manner under ATP hydrolysis conditions (Figure 6C), indicating that reduced affinity resulting from vanadate-induced trapping of nucleotide is not restricted to IAAP.

IAAP labeling of purified and reconstituted Pgp was not completely inhibited as a result of vanadate-induced trapping (Figure 5). This incomplete inhibition might be due to the mixed orientation of Pgp in proteoliposomes and the presence of inactive species in reconstituted proteoliposomes. We believe that the presence of catalytically inactive Pgp molecules can contribute to incomplete inhibition because of the following observations. Size-exclusion chromatography of Talon metal affinity purified Pgp showed that typically about 30% of the protein in a purified preparation elutes much earlier than that expected for the monomer indicating that these earlier eluting fractions represent aggregates (M. Ramachandra et al., unpublished results). We and others (*33*) have observed that the amount of this fraction increases when purified Pgp is subjected to repeated freeze−thaw cycles. Photoaffinity labeling and ATPase assays revealed that, although these aggregates retain the ability to bind drugs, they fail to bind 8-azidoATP and hydrolyze ATP (M. Ramachandra et al., unpublished results).

Inhibition of IAAP Labeling of Vanadate-trapped Pgp Only upon ATP Hydrolysis Suggests That a Conformational Change Induced as a Result of ATPase Activity Leads to Drug Release. Vanadate-induced inhibition of photoaffinity labeling occurred only when MgATP was hydrolyzed, which indicates that the resulting ternary complex consisting of Pgp, MgADP, and vanadate has a significantly reduced affinity for substrates. However, inhibition was not seen when MgATP was replaced with MgADP in the reaction (Figure 6B), suggesting that the inhibited complex does not form simply by binding of MgADP and vanadate at the catalytic site; rather, it requires ATP hydrolysis and release of phosphate. This is in contrast to the finding that a Pgp−MgADP−vanadate complex incapable of hydrolyzing ATP can be generated from exogenously added MgADP and vanadate (*21, 22*). The fact that MgADP can compete for 8-azidoATP photoaffinity labeling (Figure 3B) and can inhibit ATPase activity in a competitive manner suggests a direct interaction of MgADP at the ATP binding sites of Pgp. Therefore, it is reasonable to believe that generation of Pgp−MgADP−vanadate with a reduced affinity for substrate analogues is highly favored upon ATP hydrolysis, and its conformation is distinct from the complex that could be derived from exogenously added MgADP and vanadate.

The ternary complex consisting of Pgp, MgADP, and vanadate is believed to mimic the transition state conformation of the normal ATP hydrolysis pathway (*24*). Vanadate was previously shown to be a phosphate analogue that bound to phosphate binding sites in both myosin and dynein (*34, 35*). Recent crystal structures of the catalytic domain of myosin confirm that the ADP−vanadate complex resembles the ADP and phosphate-bound catalytic intermediate (*36, 37*). The observation that phosphate competes with vanadate during vanadate-induced inhibition of Pgp-ATPase activity further supports the idea that vanadate-trapped species mimic the normal catalytic transition state. Because phosphate binds weakly to Pgp, a very high concentration of phosphate is required for the inhibition of Pgp-ATPase activity (*21*). We were unable to demonstrate competition of phosphate for vanadate in vanadate-induced inhibition of IAAP labeling, because high concentrations of phosphate interfered with photoaffinity labeling.

In models described for P-type ATPases, changes in free energy associated with covalent E−P intermediate species generated in the catalytic cycle are believed to be coupled to alterations of both binding affinity and "sidedness" at the substrate binding sites, leading to transmembrane transport (*38*). Such a covalent E−P intermediate is not generated during the catalytic cycle of Pgp (*21*). Studies with myosin ATPase, which also does not undergo an E−P intermediate, have argued that release of phosphate triggers a profound conformational change (*39*). On the basis of the observation that phosphate binding to Pgp occurs with a relatively weak affinity, it is believed that a large decrease in free energy accompanies phosphate release (*24*). Since phosphate release has to precede formation of Pgp−MgADP−vanadate from MgATP, we propose that ATP hydrolysis and subsequent phosphate liberation induce a conformation with a low affinity for substrates that could lead to dissociation of drug from the transporter. An essential role for ATP hydrolysis and phosphate release for generation of this transition state is also supported by our findings that MgADP and vanadate failed to generate a Pgp species with low affinity for substrates (Figure 6B). It is likely that vanadate stabilizes this transient conformation by blocking the release of MgADP from the catalytic site, and in the absence of vanadate, this transient conformation is relieved with the release of MgADP. It is possible that the conformation induced upon ATP hydrolysis and phosphate release could also lead to a change in the "sidedness" of Pgp or movement of drug to the recently proposed OFF site with a relatively low affinity (*20*), which could essentially translate into drug transport.

REFERENCES

1. Gottesman, M. M., Hrycyna, C. A., Schoenlein, P. V., Germann, U. A., and Pastan, I. (1995) *Annu. Rev. Genet. 29*, 607−649.
2. Gottesman, M. M., Pastan, I., and Ambudkar, S. V. (1996) *Curr. Opin. Genet. Dev. 6*, 610−617.
3. Chen, C.-j., Chin, J. E., Ueda, K., Clark, D. P., Pastan, I., Gottesman, M. M., and Roninson, I. B. (1986) *Cell 47*, 381−389.
4. Gottesman, M. M., and Pastan, I. (1993) *Annu. Rev. Biochem. 62*, 385−427.
5. Beck, W. T., and Qian, X.-D. (1992) *Biochem. Pharmacol. 43*, 89−93.
6. Cornwell, M. M., Tsuruo, T., Gottesman, M. M., and Pastan, I. (1987) *FASEB J. 1*, 51−54.
7. Azzaria, M., Schurr, E., and Gros, P. (1989) *Mol. Cell. Biol. 9*, 5289−5297.
8. Sarkadi, B., Price, E. M., Boucher, R. C., Germann, U. A., and Scarborough, G. A. (1992) *J. Biol. Chem. 267*, 4854−4858.
9. Ambudkar, S. V., Lelong, I. H., Zhang, J. P., Cardarelli, C. O., Gottesman, M. M., and Pastan, I. (1992) *Proc. Natl. Acad. Sci. U.S.A. 89*, 8472−8476.
10. Doige, C. A., Yu, X. H., and Sharom, F. J. (1992) *Biochim. Biophys. Acta 1109*, 149−160.
11. Urbatsch, I. L., al-Shawi, M. K., and Senior, A. E. (1994) *Biochemistry 33*, 7069−7076.
12. Shapiro, A. B., and Ling, V. (1994) *J. Biol. Chem. 269*, 3745−3754.
13. Ruetz, S., and Gros, P. (1994) *J. Biol. Chem. 269*, 12277−12284.
14. Ramachandra, M., Ambudkar, S. V., Gottesman, M. M., Pastan, I., and Hrycyna, C. A. (1996) *Mol. Biol. Cell 7*, 1485−1498.
15. Horio, M., Gottesman, M. M., and Pastan, I. (1988) *Proc. Natl. Acad. Sci. U.S.A. 85*, 3580−3584.
16. Ambudkar, S. V. (1995) *J. Bioenerg. Biomembr. 27*, 23−29.
17. Sharom, F. J., Yu, X., and Doige, C. A. (1993) *J. Biol. Chem. 268*, 24197−24202.
18. Shapiro, A. B., and Ling, V. (1995) *J. Biol. Chem. 270*, 16167−16175.
19. Bruggemann, E. P., Germann, U. A., Gottesman, M. M., and Pastan, I. (1989) *J. Biol. Chem. 264*, 15483−15488.
20. Dey, S., Ramachandra, M., Pastan, I., Gottesman, M. M., and Ambudkar, S. V. (1997) *Proc. Natl. Acad. Sci. U.S.A. 94*, 10594−10599.
21. Urbatsch, I. L., Sankaran, B., Weber, J., and Senior, A. E. (1995) *J. Biol. Chem. 270*, 19383−19390.
22. Urbatsch, I. L., Sankaran, B., Bhagat, S., and Senior, A. E. (1995) *J. Biol. Chem. 270*, 26956−26961.
23. Loo, T. W., and Clarke, D. M. (1995) *J. Biol. Chem. 270*, 21449−21452.
24. Senior, A. E., al-Shawi, M. K., and Urbatsch, I. L. (1995) *FEBS Lett. 377*, 285−289.
25. Bailey, J. L. (1967) in *Techniques in Protein Chemistry*, pp 340−341, Elsevier Publishing Co., New York.

26. Germann, U. A., Chambers, T. C., Ambudkar, S. V., Licht, T., Cardarelli, C. O., Pastan, I., and Gottesman, M. M. (1996) *J. Biol. Chem. 271*, 1708−1716.
27. Hamada, H., and Tsuruo, T. (1986) *Proc. Natl. Acad. Sci. U.S.A. 83*, 7785−7789.
28. Rao, U. S. (1995) *J. Biol. Chem. 270*, 6686−6690.
29. Racker, E., Violand, B., O'Neal, S., Alfonzo, M., and Telford, J. (1979) *Arch. Biochem. Biophys. 198*, 470−477.
30. Nozaki, M., Takeshige, K., Sumimoto, H., and Minakami, S. (1990) *Eur. J. Biochem. 187*, 335−340.
31. Ambudkar, S. V., Anantharam, V., and Maloney, P. C. (1990) *J. Biol. Chem. 265*, 12287−12292.
32. Urbatsch, I. L., and Senior, A. E. (1995) *Arch. Biochem. Biophys. 316*, 135−140.
33. Loo, T. W., and Clarke, D. M. (1996) *J. Biol. Chem. 271*, 27488−27492.
34. Goodno, C. C., and Taylor, E. W. (1982) *Proc. Natl. Acad. Sci. U.S.A. 79*, 21−25.
35. Senior, A. E., Al-Shawi, M. K., and Urbatsch, I. L. (1995) *J. Bioenerg. Biomembr. 27*, 31−36.
36. Rayment, I. (1996) *J. Biol. Chem. 271*, 15850−15853.
37. Amos, L. A., and Cross, R. A. (1997) *Curr. Opin. Struct. Biol. 7*, 239−246.
38. Tanford, C. (1983) *Annu. Rev. Biochem. 52*, 379−409.
39. Spudich, J. A. (1994) *Nature 372*, 515−518.

BI973045U